# BANK EROSION PROBLEMS IN RIVER BARAK – A CASE STUDY

Fathima Israr Khan[1] and Ashim Kanti Dey[2]

[1]Research Scholar, Civil Engineering Department, NIT Silchar
[2] Professor, Civil Engineering Department, NIT Silchar
ashim_kanti@yahoo.co.in

**Abstract:** The River Barak is the second largest river in the state of Assam. It originates from the hills of Manipur and flows through three states namely, Manipur, Mizoram and Assam. It bifurcates into two parts Surma and Kushiara before entering into Bangladesh and finally discharges its water to the river Meghna. The river Barak is highly meandering and changes its course frequently, thereby, destroying the river side villages every year. Three years ago, the abutments of a bridge were constructed on both the banks of the river. During peak monsoon time, the river changed its course, destroyed one village completely and started flowing along a new route whereby both the abutments were shifted on one side. The present study includes detailed survey of the river at some other eroding location. The total station survey and bathymetric survey were carried out to obtain the cross sections of the river, geotechnical survey included borelog survey for characterizing the soil layers and geophysical survey was intended to obtain the continuous profile of the substrata. Finally, Plaxis 3D software was used to obtain the probable deformations and factor of safety of the river banks under steady state, slow draw down and rapid draw down conditions. Important conclusions were drawn at the end of the study.

**Keywords:** Geophysical Testing, Stability Analysis, PLAXIS 3D

## 1. Introduction

Meandering nature is common in alluvial rivers, especially those with a low gradient. The Barak River is a highly meandering river with a bed level difference of only 10 m over a length of 121 km between Lakhipur (the point of entering onto the plain) and Bhanga (the point of bifurcation into two tributaries). The name Barak comes from the word Bodo-Baak (Bodo-Big; Baak-Bends). The location of the river channels has changed significantly in some parts of the Barak Valley, shifting sharply north to the west of Silchar [1]. The intense meandering of the Barak River resulted in the abandonment of some loops and a general northward shift [1]. As a result of frequent cutting of riverbanks and abandonment of loops, settlements and agricultural practices are compromised, resulting in soil loss. There were many villages on the banks of the river even fifty years ago, none is visible now. Shifting of habitations from one place to another place imparts a great tragedy to the people living near the banks of the river. Soon after independence the Government constructed an embankment with boulder pitching around the Silchar city to protect it from flood and bank erosion. However, very few areas outside the city have boulder pitching.

A systematic study on causes and remedial measures of the bank erosion has not been carried out till date. Boreholes and in-situ geotechnical tests, such as the SPT, CPT, and Flat Dilatometer Test, have traditionally been used to evaluate landslides and other slope instabilities [2][3]. In addition, researchers have also suggested carrying out some specific laboratory tests like the resonant column test, ultrasonic pulse test, cyclic simple shear test, cyclic triaxial compression test, and cyclic torsional simple shear test. However, these studies, on the other hand, provide discontinuous data (limited to borehole location) and have the drawbacks of laboratory testing, such as sample disturbance, non-representative sampling, point measurements, and associated high costs. In this context, geophysical methods have emerged as a cost-effective and time-saving alternative to traditional geotechnical field testing, in addition to being non-invasive and enabling geographical and temporal investigations [4][5].

In the present study a combination of geotechnical and geophysical investigations were carried out at some selected locations where the bank erosion is continuously being taken place. Two geophysical tests namely Electrical Resistivity Tomography (ERT) and Multi-channel Analysis of Surface Waves (MASW) were carried out. The ERT gives the location of water table in the bank and the MASW gives the thickness of different layers including stiffness of the layers. Bore log soil surveys were proposed to confirm the results of the geophysical tests. Total station survey was also conducted to obtain the cross section of the river at the selected locations. Finally the stability analysis was carried out with PLAXIS-3D software [6] to obtain the factor of safety under different saturated conditions.

### 1.1 Saturation conditions of the river Barak

The banks of the river Barak experience varying degrees of submergence and drawdown every year. The banks become fully flooded during the rainy season, and when the rain stops, the water starts to draw down. As a result, the banks of the Barak River go through different stages of drawdown. For analysis three conditions have been considered namely submerged condition, rapid drawdown and slow drawdown. For rapid drawdown a period of 10 days has been considered and for slow drawdown period of 30 days has been considered.

## 2. Site Selection

Out of many erodible sites, one site at the confluence of a tributary namely Chiri was chosen for the present study. The local name of the site is Chirimukh and shifting of the river in this site from its original course is shown in Fig.1. Three locations at the Chirimukh site were selected; a photograph is also shown in Fig.2. The erosion at the banks of these three locations is shown in Fig. 3.


**Fig.1.** Google image of selected location at Chirimukh


**Fig.2.** Various selected locations at Chirimukh site

Location 1 Location 2 Location 3

**Fig.3.** Eroded Banks at three selected locations

## 3. Field work

Total station survey and bathymetric survey were carried out across the river upto the top of the bank along 10 chainages as shown in Fig. 4. A typical cross section at 620.635 m chainage is shown in Fig. 5.

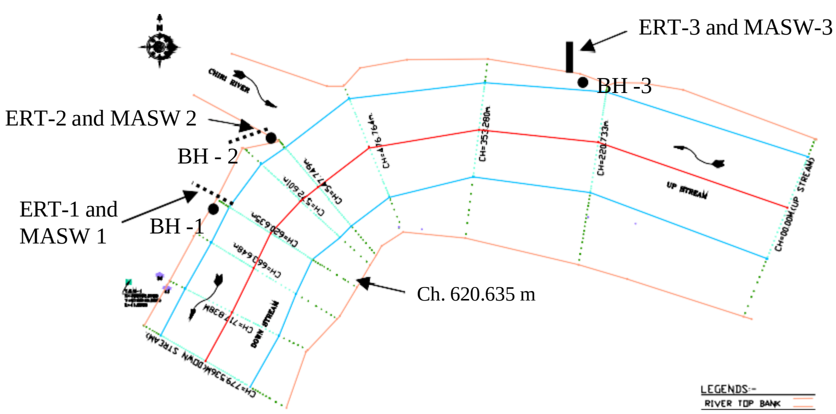


**Fig.4.** Locations of different cross sections at Chirimukh site

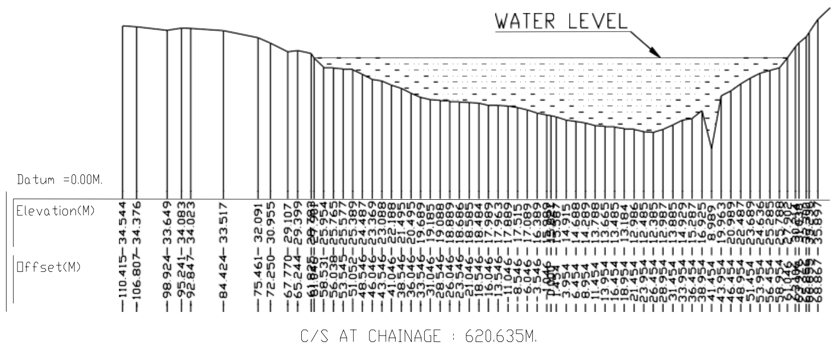


**Fig. 5** Typical cross section at chainage 620.635 m

### 3.1 Electrical Resistivity Tomography (ERT)

The electrical resistivity tomography is one of the most extensively used techniques for near-surface explorations [7]. Electrical resistivity tomography (ERT) was performed with 48 electrodes connected via a multicore cable with a resistivity meter, named Syscaljunior in which the sequence of measurements, the type of array, and other parameters like current, voltage, and the number of stacking for taking each data are saved and used. The subsequent electrodes are then automatically chosen for each measurement. The measurements are then automatically taken and are saved in the resistivity meter, which is then downloaded to a computer through Prosys II software. A variety of electrode array configurations can be used to acquire ERT data, depending on the nature of the investigation. For the present study Dipole-Dipole array was used. The apparent electrical resistivity measured in the field was inverted with the Res2dinv software (version 3.58) to assess the actual 2D resistivity model of the subsurface. The Res2dinv software is based on a smoothness-constrained least-squares optimization algorithm that enables 2D sections to be computed either using finite differences or finite elements methods [7]. The inversion occurs until the difference between the measured and the calculated values are narrowed down within a tolerable limit. The ERT data collection system is shown in Fig.6.

Fig. 6 Data collection system for ERT

### 3.2 Multi-Channel Analysis of Surface Waves (MASW)

Multi-channel analysis of surface waves (MASW) is another geophysical data collection method, andit is used to measure the ground's stiffness or elastic non properties. MASW is a destructive approach for analysing the dispersion characteristics of Rayleigh surface waves that travel horizontally [8]. Shear wave velocity measurements are useful for studying variations in subsurface stiffness [8]. In the present study, MASW surveys were performed with 24 geophones, each of a natural frequency of 4.5 Hz arranged in a linear pattern at 1m spacing. Source signals were generated by striking a steel plate with an 8 kg sledge hammer. A fixed receiver configuration was used with a shifting source point and a total of 25 shot points were used on each MASW line, one each at the middle of two consecutive geophones and one each at the either ends of the line. The raw data were analyzed using SeisImager software. Finally, the one-dimensional shear wave model was obtained by nonlinear least-squares inversion of the dispersion curve.

## 4. Field Test Results

The results of field test namely ERT and MASW conducted at all three sites are presented through figures 7 to 12:

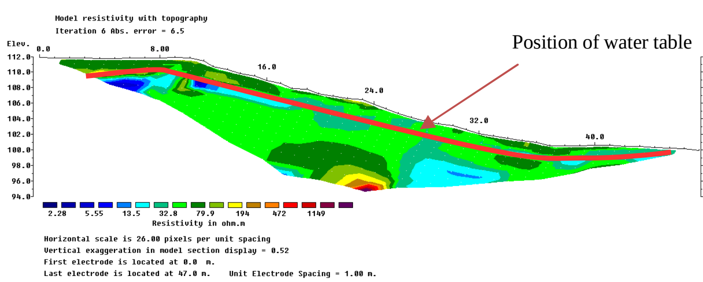


**Fig.7.** ERT 1, Location 1 - Along the slope (Dipole – Dipole)

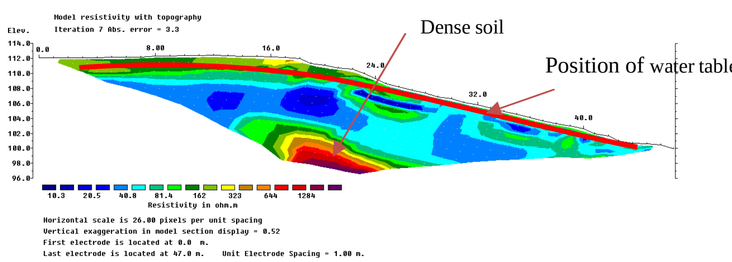


**Fig.8.** ERT 2, location 2 - Along the slope (Dipole – Dipole)

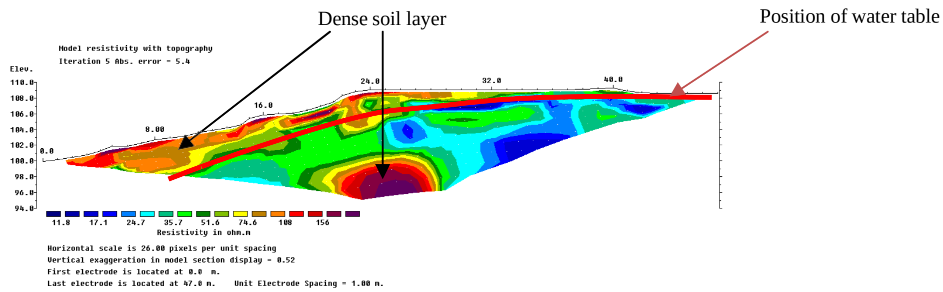


**Fig.9.** ERT 3, location – 3 - Along the slope (Dipole – Dipole)

The water table is indicated by blue layer in ERT profiles above. It also implies that the top of the light blue line may reflect soil saturated above the water table as a result of capillary rise.

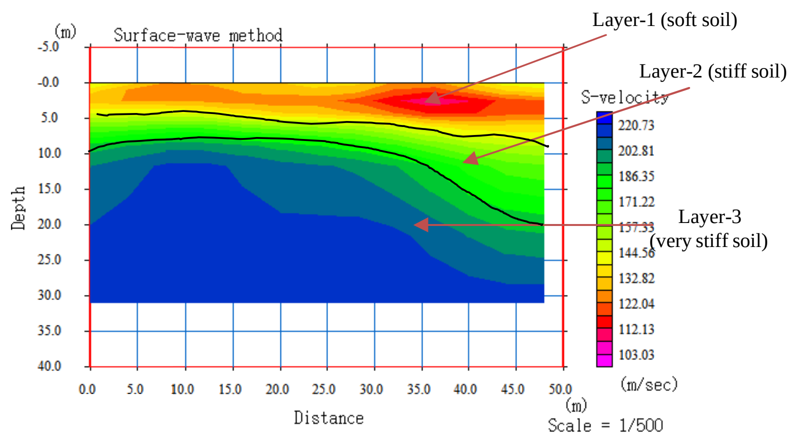


**Fig.10.** MASW -1, location 1

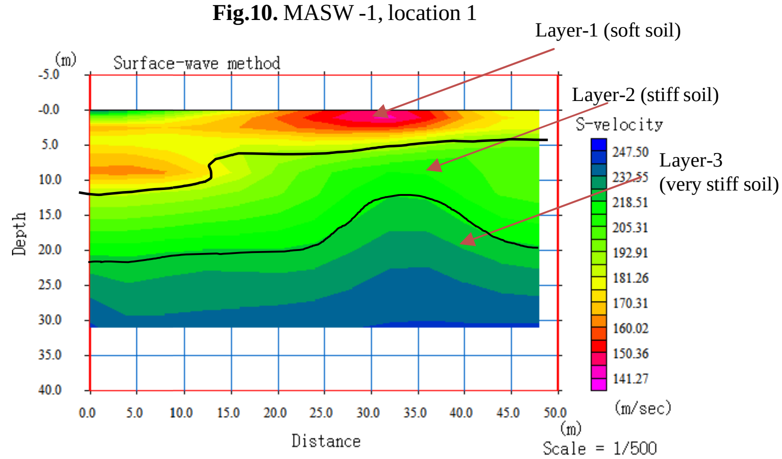


**Fig.11.** MASW 2, location - 2

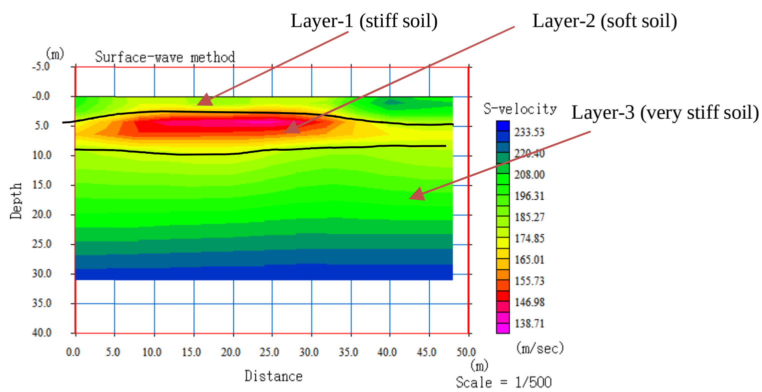


**Fig.12.** MASW 3, location - 3

## 5. Laboratory Test Results

Three bore holes were dug at the three locations as shown in Fig. 4. The samples collected from these bore holes were tested in the laboratory. The laboratory test results are shown in tabular form through tables 1 to 3.

**Table 1**: Soil Properties of BH – 1 (Location– 1)

| Depth (m) | Sand (%) | Silt (%) | Clay (%) | Dry Density (kN/m$^3$) | Saturated Density (kN/m$^3$) | c (kN/m$^2$) | φ | k (m/day) |
|---|---|---|---|---|---|---|---|---|
| 3.00 | 15.96 | 76.22 | 7.82 | | | | | |
| 4.50 | 22.45 | 68.09 | 9.46 | 15.50 | 18.50 | 10 | 22 | 0.0055488 |
| 6.00 | 20.17 | 70.96 | 8.87 | | | | | |
| 7.50 | 10.24 | 77.81 | 12.57 | | | | | |
| 9.00 | 12.71 | 71.42 | 15.87 | 16.70 | 19.00 | 12 | 24 | 0.0045705 |
| 10.50 | 10.46 | 75.61 | 13.93 | | | | | |
| 12.00 | 15.73 | 72.51 | 11.76 | | | | | |
| 13.50 | 30.97 | 56.19 | 12.84 | 18.80 | 20.00 | 15 | 18 | 0.008227 |
| 15.00 | 37.90 | 50.21 | 11.89 | | | | | |

**Table 2**: Soil Properties of BH – 2 (Location– 2)

| Depth (m) | Sand (%) | Silt (%) | Clay (%) | Dry Density (kN/m$^3$) | Saturated Density (kN/m$^3$) | c (kN/m$^2$) | φ | k (m/day) |
|---|---|---|---|---|---|---|---|---|
| 1.50 | 10.47 | 76.22 | 7.82 | 15.59 | 17.72 | 6 | 27 | 0.001466 |
| 6.00 | 6.46 | 77.95 | 15.59 | | | | | |
| 9.00 | 4.73 | 77.41 | 17.86 | 16.02 | 18.89 | 15 | 25 | 0.0006912 |
| 12.00 | 9.78 | 72.57 | 17.65 | | | | | |

**Table 3**: Soil Properties of BH – 3 (Location– 3)

| Depth (m) | Sand (%) | Silt (%) | Clay (%) | Dry Density (kN/m$^3$) | Saturated Density (kN/m$^3$) | c (kN/m$^2$) | φ | k (m/day) |
|---|---|---|---|---|---|---|---|---|
| 1.50 | 37.36 | 51.25 | 11.39 | | | | | |
| 3.00 | 42.76 | 47.70 | 9.54 | 15.61 | 18.65 | 5 | 25 | 0.0099809 |
| 4.50 | 35.70 | 53.58 | 10.72 | | | | | |
| 6.00 | 47.43 | 43.14 | 9.44 | 14.22 | 17.59 | 10 | 20 | 0.0027648 |
| 9.00 | 49.49 | 36.08 | 14.43 | 16.62 | 18.98 | 18 | 12 | 0.0022394 |
| 10.50 | 27.46 | 60.23 | 12.31 | | | | | |

## 6. Analytical Study

### 6.1 Geometry

The geometry of various slopes created from MASW results and Borehole data are as follows ( Fig. 13):

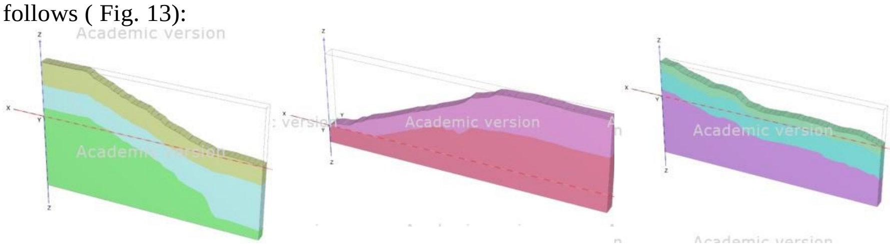


**Fig.13.** Created Geometry for slope at locations-1, 2 and 3

### 6.2 Water Levels

Two water levels are created for each slope one representing the water level in submerged condition and the other representing the water level in the driest condition as shown in Fig. 14.

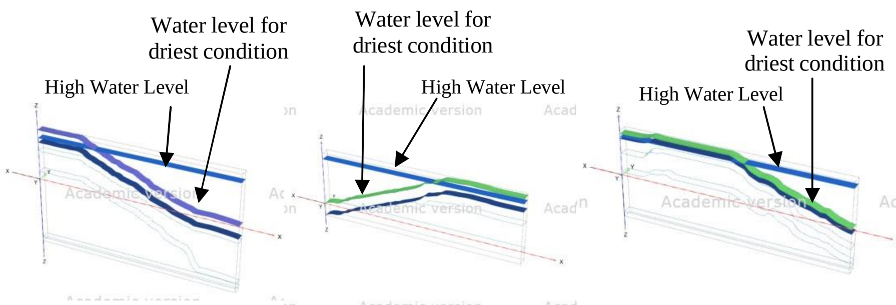


**Fig.14.** Created water levels for slope at locations-1, 2 and 3

### 6.3 Analysis

The analysis was carried out with Plaxis 3D software. The analysis is done with initial phase as river full condition or submerged condition. The next phase is rapid drawdown phase in which different values of head drop is considered and the Factor of Safety, FOS is calculated corresponding to each head drop. The last phase is the slow drawdown phase in which a period of 30 days is assigned to different values of head drop and corresponding to that FOS has been calculated.

## 7. Results

The deformed mesh after the rapid drawdown at the three locations are shown in Fig.15. The deformations at different stages of water table variations are shown in Figs. 16 to 18. The FOS for different locations of water table are shown in Table 4.

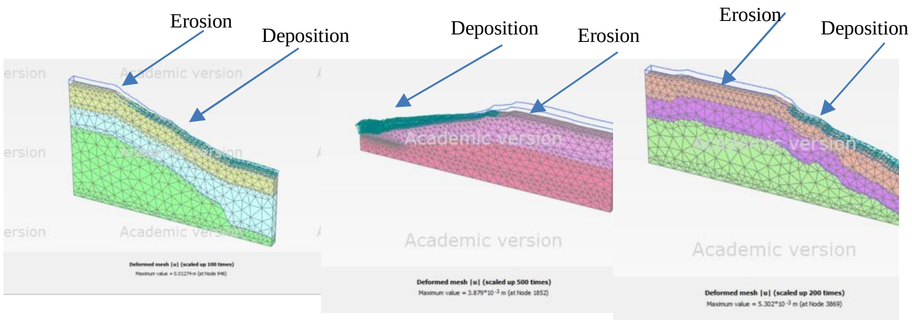


**Fig.15.** Deformed Mesh

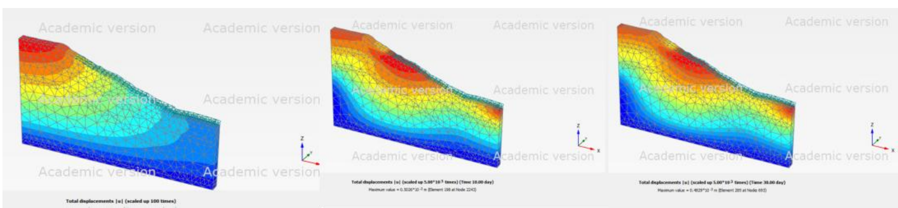

**Fig.16.** Deformation during submerged, rapid and slow drawdown for 1 m head drop for location-1

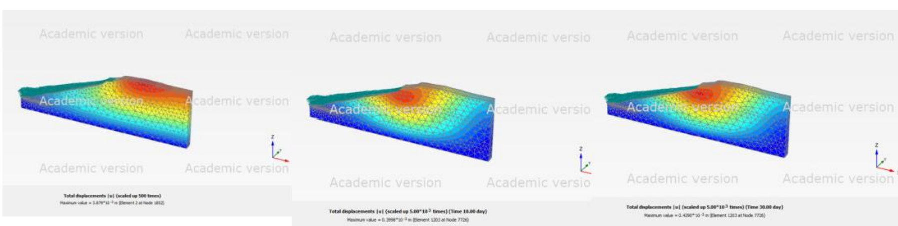

**Fig.17.** Deformation during submerged, rapid and slow drawdown for 1 m head drop for location-2

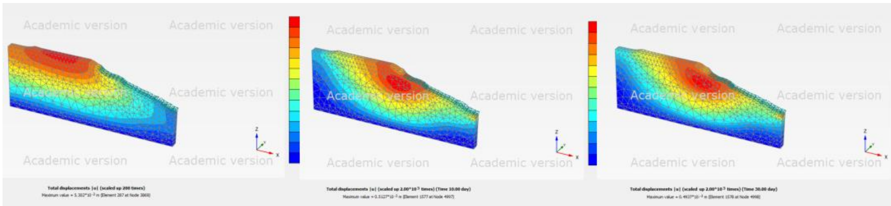

**Fig.18.** Deformation during submerged, rapid and slow drawdown for 1 m head drop for location-3

**Table 4**: Factor of Safety of three sites for rapid and slow drawdown

| Head Drop (m) | Factor of Safety | | | | | |
|---|---|---|---|---|---|---|
| | Location - 1 | | Location- 2 | | Location - 3 | |
| | Rapid Draw down | Slow Drawdown | Rapid Drawdown | Slow Drawdown | Rapid Drawdown | Slow Drawdown |
| 1.00 | 1.710 | 1.716 | 1.872 | 1.889 | 1.882 | 1.889 |
| 1.50 | 1.606 | 1.615 | 1.704 | 1.785 | 1.713 | 1.728 |
| 2.00 | 1.511 | 1.543 | 1.663 | 1.672 | 1.594 | 1.627 |
| 2.50 | 1.444 | 1.478 | 1.558 | 1.560 | 1.510 | 1.542 |
| 3.00 | 1.368 | 1.389 | 1.449 | 1.458 | 1.363 | 1.378 |
| 3.50 | 1.302 | 1.325 | 1.363 | 1.378 | 1.296 | 1.313 |
| 4.00 | 1.252 | 1.272 | 1.299 | 1.311 | 1.241 | 1.251 |

## 8. Discussion and Conclusions

The FOS values for rapid and slow drawdown conditions are quite comparable, however, the factor of safety is little more for slow drawdown case. The slope is becoming more unstable when the value of head drop is increased. It is also observed from the Plaxis analysis that the slope is not failing; however, there is soil erosion from the top after the draw down case. Similar problem was observed in the site also as observed in Fig.3. Soil from the top erodes down after every flood. At some locations the slope becomes near vertical at the top which is susceptible to collapse in the next monsoon. This analysis will be carried out in the future study.

## References

1. Das, J. D., Dutta, T. and Saraf, A. K. Remote sensing and GIS application in change detection of the Barak River Channel, N. E. India. J. of the Ind. Soc. of Rem. Sens., 35, 301-312 (2007)
2. Hamza, O. and Bellis, A. Gault clay embankment slopes on the A14- Case studies of shallow and deep instability. 1st International conference on Transportation Geotechnics, DOI 10.1201/9780203885949.ch40 (2008).
3. Mitchell R.J. On the retrogression of landslides in sensitive muddy sediments. Canadian Geotechnical Journal, 15 (3) (1978).

4. Taipodia, J., Baglari, D., Dey, A. Effect of Source Characteristics on the Resolution of Dispersion Image from Active MASW Survey. Indian Geotechnical Journal 49, 314–327. https://doi.org/10.1007/s40098-018-0335-1 (2019).
5. Bery, A.A., Ismail, N.E.H and Muztaza. Soil Properties and Behaviour Studies using Joint-interpretation of 4-D Electrical Resistivity Tomography and Soil Mechanics Methods in Penang, Malaysia. 2nd Asia Pacific Meeting on Near Surface Geoscience and Engineering, https://doi.org/10.3997/2214-4609.201900402 (2019).
6. Bentley "PLAXIS 3D-CE-V2-2.00-2-Reference" (2020)
7. Loke, M.H., Wilkinson, P.B., Chambers, J.E., Meldrum, P.I.. Rapid inversion of data from 2D resistivity surveys with electrode displacements. Geophysical Prospecting 66, 579–594. https://doi.org/10.1111/1365-2478.12522 (2018)
8. Park, C.B., Miller, R.D., Xia, J. Multichannel analysis of surface waves (MASW). Geophysics 64. https://doi.org/10.1190/1.1444590 (1999).